Journal of African Earth Sciences 100 (2014) 267–277

Contents lists available at ScienceDirect

Journal of African Earth Sciences

journal homepage: www.elsevier.com/locate/jafrearsci

Mineralogical and geochemical signatures of clays associated with rhyodacites in the Nefza area (northern Tunisia)

D. Sghaier [a,*], F. Chaabani [a], D. Proust [b], Ph. Vieillard [c]

[a] Laboratoire de Ressources Minérales et Environnement, Université de Tunis El Manar, Faculté des Sciences de Tunis, Département de Géologie, Campus Universitaire, 2092 Tunis, Tunisia
[b] LIENSs-UMR 7266 CNRS, Université de La Rochelle, 2 rue Olympe de Gouges, 17000 La Rochelle, France
[c] HYDRASA-UMR 6532 CNRS, Université de Poitiers, 40, avenue de Recteur Pineau, 86022 Poitiers, France

ARTICLE INFO

Article history:
Received 19 November 2013
Received in revised form 26 May 2014
Accepted 2 June 2014
Available online 19 July 2014

Keywords:
Alteration
Hydrothermalism
Oued Belif
Rhyodacite
Smectites
REE

ABSTRACT

The geology of northern Tunisia is marked by magmatic extrusion that occurred during the Middle Miocene (Langhian–Lower Tortonian), which led to the outcrops of rhyodacites in the Nefza-Tabarka region. This event is contemporaneous with the Alpine compressional phase, which is well-characterised in the western Mediterranean area, where intense fracturing and hydrothermalism occurred with evidence of metallogenic consequences.

In this paper, a detailed study is presented on the acid volcanic rocks that outcrop at the core of the Oued Belif structure in the Nefza area of northern Tunisia. The results indicate that these series have undergone various transformations subsequent to their extrusion. These alterations include ferrugination, silicification, argilitisation and devitrification of volcanic glass.

Petrographic observations demonstrated that the primary minerals, particularly feldspars, biotite and mesostasis glass, were affected by hydrothermal and meteoric weathering. The mineralogical study of the neogenic products revealed a nearly monomineral smectitic phase with relatively low levels of added illite and/or kaolinite. These neoformed smectites were classified as ferroan beidellites–nontronite based on thermal and crystallochemical analyses. Chemical analysis of the major elements, trace elements and rare Earth elements (REEs) show the presence of Al, Fe and K and an enrichment of REE in the clay fraction with a greater fractionation of light rare Earth elements (LREEs) compared with that of heavy rare Earth elements (HREEs). The abundance of these elements is attributed to their mobility during chemical weathering of acidic lavas and their adsorption by clay minerals.

1. Introduction

Previous studies on the weathering of volcanic rocks have demonstrated that the most common neoformed mineral is smectite, which is typically associated with illite and kaolinite. These neogene minerals are formed either by hydrothermal alteration or through supergene alteration of acidic or basic lavas (Grim and Güven, 1978; Meunier et al., 1984). Weathering affects primary minerals, such as feldspars, biotites, pyroxenes and mesostasis glass. The alteration products are closely related to the nature of the parent rock and the physicochemical characteristic of the geological environment, such as the transformation agent and the weathering intensity (Christidis, 1998; Ddani et al., 2005). This relationship has been observed in many bentonite deposits associated with volcanic rocks, such as in Trébia, Afrah and Ikasmeouen in Morocco (Ddani et al., 2005) and in Maghnia and Mostaghanem in Algeria (Abdelouahab et al., 1988). In the eastern extension of these north African volcanic provinces (i.e., the Nefza region of northern Tunisia), smectitic minerals have been reported as secondary products of the rhyodacite dome and its related pyroclastic flows or ash fall deposits (Dermech, 1990; Moussi, 2012; Sghaier, 2005; current study). This region presents a suitable environment for the neoformation of smectite by hydrothermal alteration and/or a meteoric alteration process.

The present paper discusses the results obtained from petrographic, mineralogical and crystallochemical studies of the Oued Belif rhyodacites and the identification of their mineralogical and geochemical responses to meteoric and hydrothermal alterations associated with magmatic activity. In addition, this study attempts to characterise the variation of the crystalline structure of smectite

* Corresponding author. Tel.: +216 24092580; fax: +216 71751261.
E-mail address: sghaier.dalel@gmail.com (D. Sghaier).

http://dx.doi.org/10.1016/j.jafrearsci.2014.06.024
1464-343X/

(as an alteration product) based on the physicochemical characteristics of the geological environment.

In the North African margin, the Miocene period corresponds to a compressive phase, which is typically known as the Alpine phase (Last Burdigalian–Early Serravalian) related to the convergence of the African and Euroasian plates (Tlig et al., 1991). This collision led to the southward overthrusting of the internal zone onto the African passive margin (Late Burdigalian–Langhian), the latter of which was deformed into a fold and thrust to later create the Tellian Zone during the Early Serravallian–Tortonian. This stage coevals with the Sardinia counter-clockwise rotation that led to the drifting stage of the Algiers-Provence West Mediterranean oceanic basin with an initial aperture in the Late Oligocene–Aquitanian (Cohen et al., 1980; Jolivet and Faccenna, 2000; Tlig et al., 1991).

A subsident perimediterranean basin was consequently formed and filled by the Late Oligocene–Early Burdigalian Numidian Flysch (a thick silicoclastic turbidite formation), which was overthrusted to the south onto the Tellian Zone at the end of the Burdigalian (Ould Bagga et al., 2006; Riahi et al., 2010; Rouvier, 1977). Post-dating of the thrusting, several of the volcanic rocks were emplaced along the faulted area (Dermech, 1990; Halloul, 1989; Laridhi Ouazaa, 1994; Mauduit, 1978; Negra, 1987; Rouvier, 1977; Talbi, 1998; Talbi et al., 2005). The last recorded magmatic activities in north Tunisia occurred during the Miocene–Basal Pliocene with a transition of calc-alkaline acid rocks to subalkaline and alkaline basic rocks (Bagdazarjan et al., 1972; Faul and Foland, 1980). The acid rocks primarily occurred in the Galite and Nefza-Tabarka regions during the Langhian to Lower Tortonian (15–8 Ma). On Galite Island, intrusive granitoids are composed of granodiorite, microgranite and granitic aplite. However, in the Nefza-Tabarka region, there are small-scale outcrops that include domes and flows of granodiorite (Ragoubet el Alia), rhyodacite (Ragoubet Es Seid, Aïn Deflaîa and Jebel Haddada) and Oued Zouara pyroclastics (Fig. 1). These acidic rocks are associated with basaltic sills and dykes that occurred during the Upper Tortonian–Messinian (8–5.8 ± 1 Ma) and outcrop in the localities of Boulanague and Mogods. Recently geophysical studies have shown that the extent of the subsurface igneous bodies beneath the Numidian nappes is actually larger than the area occupied by the outcropped volcanic rocks (Jallouli et al., 1996).

In both the surface and subsurface, these igneous rocks have undergone transformations subsequent to their emplacement. Previous studies have shown that post-magmatic alteration is extremely advanced in the pyroclastic rocks (Halloul, 1989; Laridhi Ouazaa, 1994), granodiorites (Dermech, 1990; Halloul, 1989; Kasaa et al., 2003; Negra, 1987; Talbi, 1998) and rhyodacites but is moderate in the basaltic lavas (Halloul, 1989; Laridhi Ouazaa, 1994; Negra, 1987; Talbi, 1998).

The acidic lavas and their pyroclastics have been frequently altered by fumaroles and hydrothermal circulation (Mauduit, 1978; Negra, 1987). As a result, the volcanic glass has been devitrified and transformed into phyllosilicates (Negra, 1987). However, the nature of the secondary phyllosilicates remains to be determined, and their crystallochemical characteristics have not been intensively studied until now. Therefore, this present work focuses on reviewing the clayey transformations undergone by the rhyodacites of Ragoubet Es Seid, which is located in the core of the Oued Belif structure.

2. Geological setting

The study area (Oued Belif) is located in the Nefza window that separates the Mogods and the Kroumirie mountains (Rouvier, 1987). This area is limited to the south by Ed Diss jebel (Fig. 1), where Rouvier (1977) defined the Ed Diss Tellian units (Upper Cretaceous to Eocene). This unit consists of alternating marls and limestones and is overlain by the so-called Numidian Flysch. The latter consists of approximately 3000 m of alternating turbiditic sandy and clayey formation of Oligocene–Lower Miocene age (Riahi et al., 2010; Rouvier, 1977; Yaich, 2000). In the north, the Oued Belif structure is bordered by two small post-nappe basins (the Sidi Driss–Tamra basins) which host minor Pb–Zn–Fe ores (Bouzouada, 1992; Decrée et al., 2008a, 2008b; Dermech, 1990; Doumbouya, 1999; Gottis, 1952; Gottis and Sainfeld, 1952; Sainfeld, 1952).

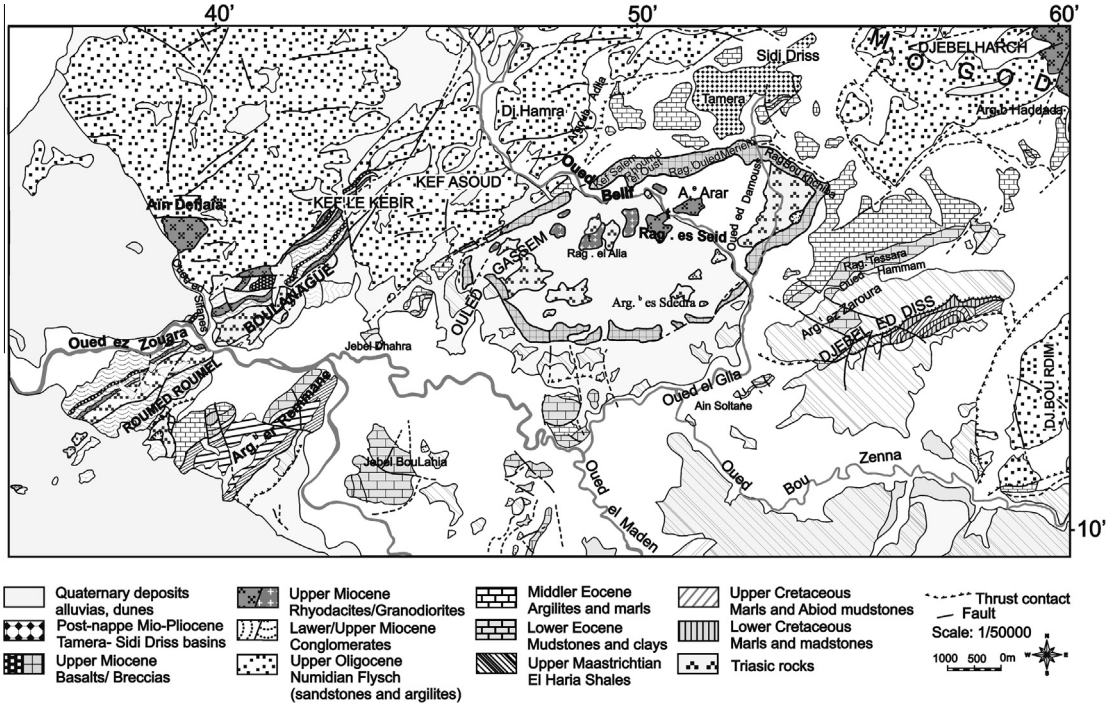

Fig. 1. Geological sketch map of the studied area (modified and redrawn from Rouvier, 1977).

The Oued Belif area represents a deep-rooted structure shaped in an oval of approximately 6 × 3 km, which fits perfectly within the Upper Miocene ferruginous breccias (Fig. 1). The area encloses several outcrops of post-Miocene volcanic (rhyodacite) rocks, intrusive lava (granodiorite), saliferous Triassic rocks (magmatic host rocks) and skarn deposits, which are outlined by a ferruginous breccia (Bellon, 1976; Chaftar, 1997a,b; Decrée et al., 2013; Gottis and Sainfeld, 1952; Halloul, 1989; Mauduit, 1978; Perthuisot, 1978; Rouvier, 1977, 1987, 1988). These extrusive bodies pierce the allochthonous cover. The extrusive rocks are represented by the rhyodacite domes of the Ragoubet Es Seid. Numerous flows are derived from the base of this dome and reveal extrusive breccias. These breccias contain millimetre- to centimetre-scale subspherical to angular blocks of highly altered rhyodacites and reworked elements of saliferous rocks, which are cemented by a siliceous matrix. Mylonitic banding has also been observed at the level of these breccias, providing evidence of a late fumarolic activity (Mauduit, 1978). The interaction between the lava and the Triassic host rock could intervene in the brecciation processes of the lava and in its impregnation with ferric oxide.

Another notable feature of this structure is its location in the mining province of Tamra (iron) and Sidi Driss Dhouahria Boukhchiba (Pb–Zn) (Decrée et al., 2008a,b). The establishment of this mineralisation is linked to the magmatic activity and hydrothermal fluids (Decrée et al., 2008a,b; Dermech, 1990; Halloul, 1989; Negra, 1987; Talbi, 1998; Talbi et al., 1999, 2005). This complex structure has been interpreted as a volcanic caldera (Talbi, 1998) and is also mostly attributed to significant hydrothermal activity (Dermech, 1990; Talbi, 1998). Talbi (1998) stated that the hydrothermal alteration was porphyritic in depth and epithermal "acid-sulphate-like" in shallow areas. This hydrothermal alteration is evidenced by several processes, such as argillic alteration, chloritisation, albitisation, propylitisation, carbonation, tourmalinisation and silicification (Talbi, 1998). In contrast, Crampon (1971) and Mauduit (1978) considered that this complex structure is a salt diapir associated with magmatism.

3. Materials and methods

Magmatic rock samples were collected from the Oued Belif structure and from the immediate surrounding geological units.

X-ray diffraction (XRD) was performed on both randomly oriented powders and oriented preparations of three different states: air-dried (AD) samples, ethylene glycol-solvated samples using a 60 °C vapour phase (EG) and samples heated to 500 °C (HAD). The XRD patterns were recorded using a PANalytical X'Pert PRO X-ray diffractometer equipped with an automatic slit, Xcelerator and Cu Kα radiation, which used a Ni-filter and was generated at 40 kV and 40 mV.

Scans were using an angular range of 2–30°2 θ, a step size of 0.025°2 θ and a counting time of 4 s for the oriented preparations; for the randomly oriented powders, an angular range of 5–65°2 θ, a step size of 0.025°2 θ and a counting time of 8 s were used.

The chemical analyses, texture and composition of the rock samples and clay minerals were examined using a JEOL JSM-5600LV scanning electron microscope (SEM) coupled with an energy dispersive spectrometer (EDS) (Bruker AXS Microanalysis) at Poitiers University. The analyses were performed on pressed and carbon-coated pellets.

The major elements were measured from both the bulk rock and clay fraction (<2 μm) using inductively coupled plasma-emission spectroscopy (ICP-ES). The concentrations of trace elements, including REEs, were determined by inductively coupled plasma-mass spectroscopy (ICP-MS) at the Centre de Recherches Pétrographiques et Géochimique (CRPG) in Vanoeuvre-lès-Nancy (France). Chemical analyses of the major, trace and REEs were performed using the $LiBO_2$ fusion method for powdered rocks followed by dissolution in HNO_3 acid.

The structural formula was calculated based on the $O_{10}(OH)_2$.

Infrared spectroscopy was performed on pressed pellets using a KBr beamsplitter and a DTGS/KBr detector on a Nicolet 510 FTIR spectrometer.

The pellets were prepared by mixing 1 mg of sample with 150 mg of well ground KBr. The mixture was then pressed for 5 min at 5 tons and 4 min at 12 tons. The prepared pellets were placed in oven, which was maintained at 110 °C overnight prior to the analyses. Middle infrared (MIR) spectra were recorded between 4000 and 400 cm^{-1}.

Differential and thermogravimetric analyses were obtained using a SETARAM SETSYS-1750 instrument operating in helium atmosphere and heated at a rate of 10 °C/min to a maximum temperature of 1000 °C.

4. Results

4.1. Petrographic and mineralogical study of rhyodacites

The macroscopic and microscopic examination of the rhyodacite samples of the Oued Belif shows that they are of green–grey in colour when unweathered and become red or yellow patina when weathered. The rhyodacite samples have a microlitic texture and contain plagioclase phenocrysts (often zoned), sanidine (occasionally with Carlsbad twinning), biotite, quartz, apatite, zircon, monazite, opaque vitreous minerals with a pearlitic matrix and colourless mesostasis glass. These lavas occur regularly in a highly altered state (Fig. 2), which is supported by the fact that the structure of the original rock is not preserved as well as the occurrence of ferruginous weathered products of biotite, opaque minerals and glass (Fig. 2). The latter can be fresh or devitrified and altered (Fig. 3B). The quartz crystals are deeply corroded by mesostasis and show a rhyolitic quartz aspect (Fig. 2A). Biotite crystals are either euhedral, fractured, corroded and/or lightly leached and show cleavage planes that have been frequently oxidised (Fig. 2B and D). Locally, several of the biotite crystals are pseudomorphised into phlogopites or partially chlorotised (Dermech, 1990; Talbi, 1998). Feldspars are intensively altered (Fig. 2B–D). Additionally, several dissolution cavities that affect the plagioclase crystals were observed using optical microscopy and SEM (Fig. 3). These pores are filled by neoformation products, such as phyllosilicates and iron oxides (Figs. 3 and 4). In addition to the ferruginisation and argilitisation, intense silicification also affected these acid rocks. This silicification is clearly evident at both the northern and northwestern borders of the Ragoubet Es Seid dome. In the upper part of this dome, Negra (1987) identified a weathering sequence at the rhyodacite consisting of three horizons: bed rock, saprolite and an upper clayey horizon, which is primarily composed of beidellite with a small amount of kaolinite. In the Ragoubet el Alia, the granodiorites were also weathered. The late- or post-magmatic circulation of hydrothermal fluids provoked the albitisation of K-feldspar and the sericitisation or tourmalinisation of biotite in the granodiorite (Dermech, 1990; Talbi, 1998).

4.2. Mineralogical study of clays from rhyodacites

The mineralogical study of the fine fraction extracted from the poorly preserved samples shows that the mineral assemblage primarily consists of smectite, illite and traces of kaolinite (Figs. 5 and 6). The swelling phase represents the major fraction (>90%). Pure smectitic phases have been preferentially encountered in the weathered lava adjoining the Triassic sedimentary formations

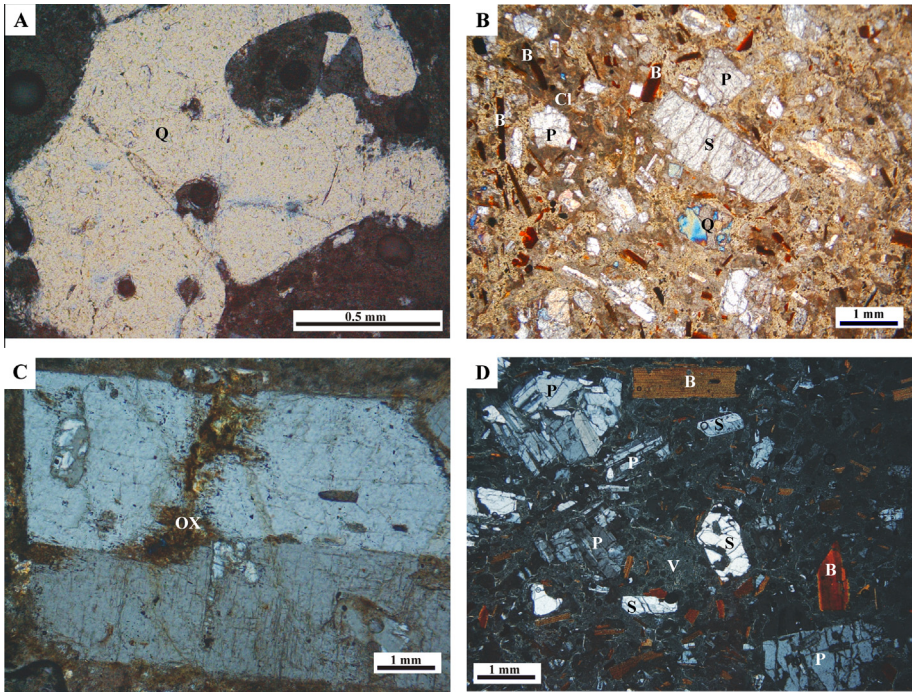

Fig. 2. Images of thin sections of Nefza volcanic rocks observed under a polarised microscope. (A) Rhyolitic quartz deeply corroded by mesostasis. (B) Brown glass present as an interstitial phase. (C) Sanidine phenocryst with simple twinning and a size of up to 8 mm size; phenocrysts exhibit dissolution cavities filled with clays and iron oxides. (D) Partly devitrified microlitic porphyric texture with transparent glasses. Zoned Plagioclase phenocrysts set in a fine matrix of biotite laths.

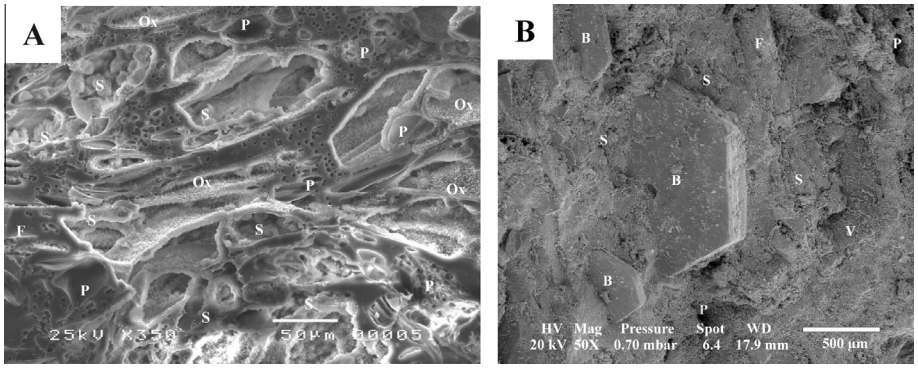

Fig. 3. (A) Scanning electron microscopy (SEM) photomicrograph showing a crystal of feldspar that has dissolution pores indicative of weathering. The empty spaces are partially filled with oxides and neoformed clays. S: smectitic clays; P: dissolution pores; Ox: oxide; F: feldspar. B: SEM image showing euhedral crystals of biotite (B) lined by clays, all of which are contained within a siliceous groundmass (volcanic glass). Neoformed clays (S) obtained from the transformation of volcanic glass (V) and the dissolution of feldspars (F); (P): pores.

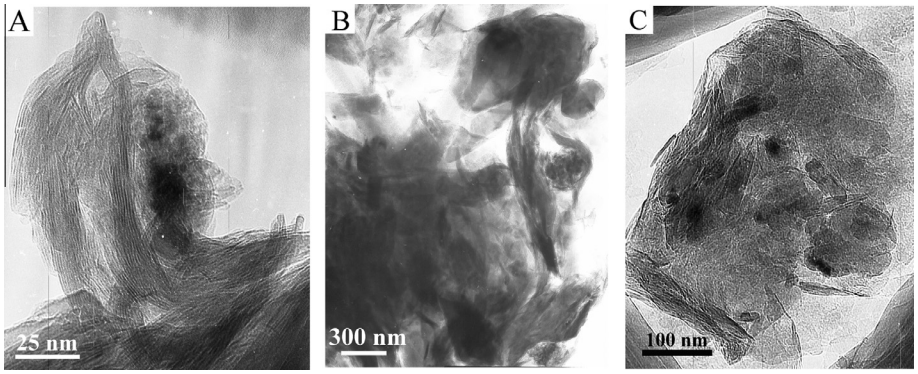

Fig. 4. TEM images showing iron oxides adsorbed on the surface of the clays (A and B) and in the intrastructural micropores (C).

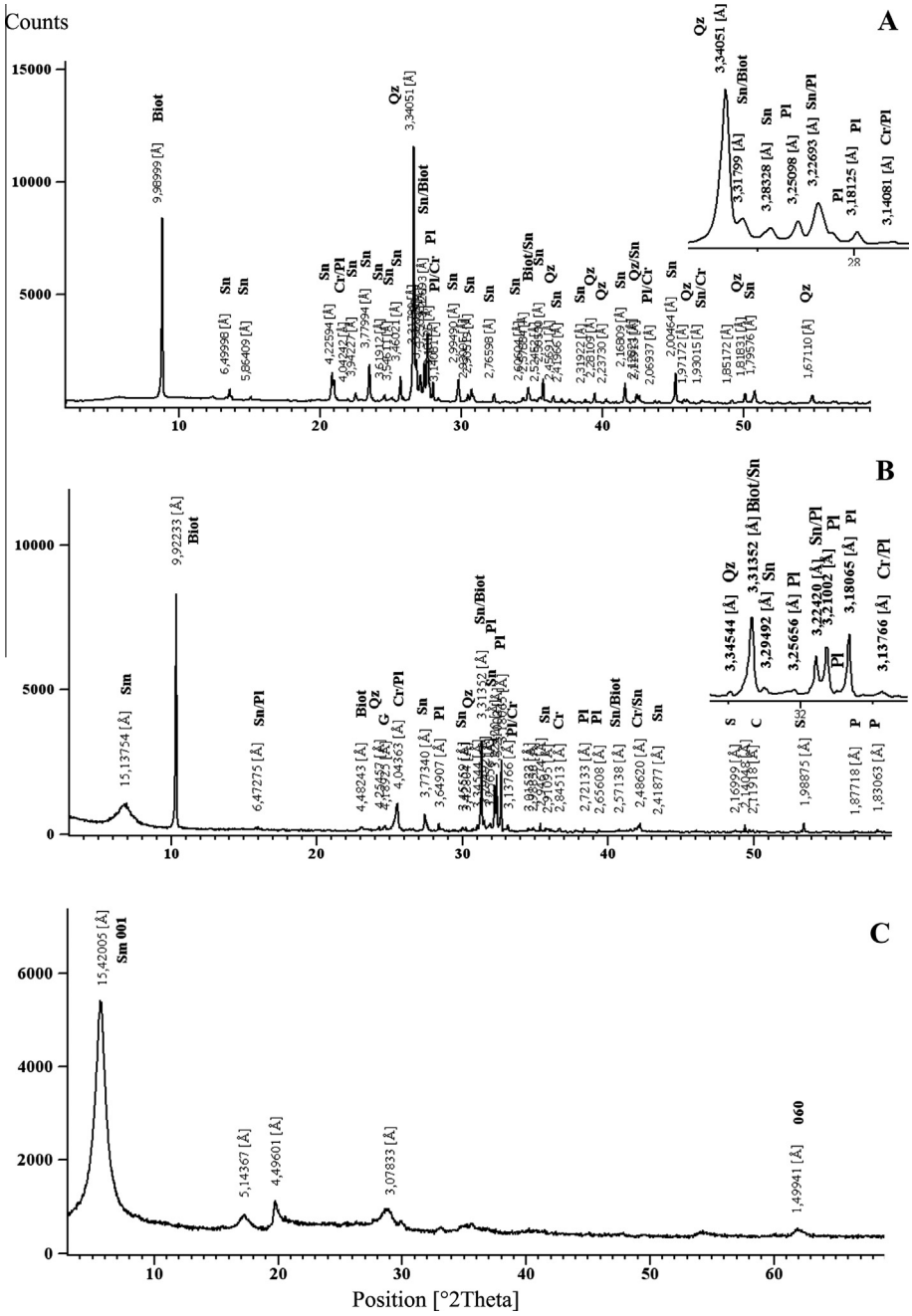

Fig. 5. XRD patterns of randomly oriented powders of the fresh bulk (A), altered rock (B) and clay fraction (C) of the Oued Belif samples. Sm: smectite, Biot: biotite, G: goethite, Cr: cristobalite, Qz: quartz, Sn: sanidine, Pl: plagioclase.

and the volcanic rocks. At this level, the facies have a dark rose to red tint, which is comparable to that of the Tamra Formation and the Triassic red clays, which progressively evolve to a light yellow-to-grey tint as the rock becomes fresh. The obtained powder diffraction diagrams are within the <2 micron fraction, which has an interplanar distance band of (0 6 0) close to 1.49 Å and confers a dioctahedral character (Fig. 5). The micaceous phase represented by the illitic minerals does not exceed 10% of the entire clay fraction. The kaolinite appears sporadically.

4.3. Crystallochemical study

To determine whether the smectites are montmorillonitic or beidellitic clays, the charge of the dioctahedric clays was neutralised by the migration of a small cation (lithium) in the unoccupied octahedral cavities by heating to 250 and 300 °C (Hofmann and Klemen, 1950; Schultz, 1969; Fig. 6). The Hofmann–Klemen effect showed that highly weathered samples (from the volcano-sedimentary breccia) correspond to an intermediate phase between the montmorillonitic and beidellitic poles (Fig. 6A). The Hofmann–Klemen treatment that was performed on less weathered samples showed two peaks, at 17 Å and 8.74 Å, which are indicative of beidellitic sheets. The intensity of the peak at 9.95 Å was invariant after lithium treatment, which excludes the presence of montmorillonitic smectite (Fig. 6B). Regarding the least-weathered samples (collected nearest to the fresh rock), the swelling sheets dominated with a relatively significant illitic proportion (Fig. 6C). The lithium saturation resulted in two peaks at 17 Å and 8.74 Å, which supports the presence of beidellitic sheets, whereas the 9.96 Å peak matches a dual micaceous and smectitic dual stage.

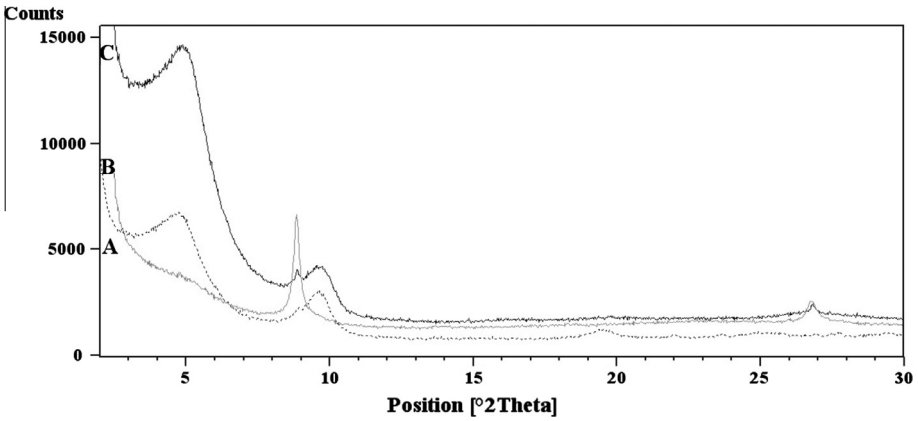

Fig. 6. XRD spectrum of the <2-μm fraction of the Oued Belif samples after Hofmann–Klemen treatment (A: OB3 (grey solid line), B: OB6 (black dots) and C: OB24 (black solid line)).

This peak includes both illitic and montmorillonitic layers due to its increased intensity compared with that observed prior to the lithium treatment.

The sheet charge of the phyllosilicates was determined using the sample saturation process with Ca and Ca–K followed by Ca–K–Ca (Sato et al., 1992; Fig. 7). The first calcium saturation of the most distal samples (Fig. 7A) revealed the presence of mono-mineral smectite.

The same preparation saturated with K exhibited heterogeneity in the distribution of the sheets: highly charged sheets behaved like micaceous minerals, which were then heated at ~110 °C and remained closed at 10 Å after re-saturation with Ca^{2+} and ethylene glycol (Fig. 7A); and poorly charged sheets (12 Å) shifted to 15 Å after the second Ca^{2+} saturation and swelled in the presence of ethylene glycol. Therefore, this sample includes two types of smectite with at different proportions: montmorillonite (dominant) and beidellite. Regarding the less-altered-samples (Fig. 7B and C), the interfoliar spaces folded down to 12 Å after successive saturations with Ca and K and then shifted to 15 Å during the second Ca^{2+} saturation. The potassium ions that are weakly adsorbed on sheets were completely removed by the Ca^{2+} cations.

The values of the cation exchange capacity (CEC) and surface area values determined using the Brunauer, Emett and Teller method (BET) are given in Table 1. The CEC, which was measured at a pH of 7, ranged from 61 to 79.2 meq/100 g, which is less than the CEC of smectites (60–120 meq/100 g). Furthermore, the specific surface area measured by nitrogen adsorption ranged between 53.14 and 80.08 m^2/g.

4.4. Infrared spectroscopy

The cation distribution in both the octahedral and tetrahedral layers of the clays identified by XRD, were determined by IR spectroscopy with hydroxyl linking.

The IR spectra revealed intense bands at 3628 cm^{-1} (Fig. 8), which are attributed to the AlAlOH stretching vibration of beidellitic smectite (Petit et al., 1995). The band at 883 cm^{-1} is attributed to the $AlFe_3OH$ bending vibration, and the 524 cm^{-1} band matches the SiOAl bending vibration. The band at 467 cm^{-1} coincides with the SiOMg bending vibration. The farthest samples from the rhyodacitic dome have stretching vibrations bands of hydroxyl groups and deformation bands, which are characteristic of a smectite-like mixed with a single Wyoming beidellitic component. The IR spectra of the least-altered samples collected near the fresh rock (i.e., OB24) revealed that the valence vibrations field included hydroxyl groups and AlAlOH deformation bands δ (Al_2OH) and δ (OHAlFe) at 3630 cm^{-1}, 923 cm^{-1} and 881 cm^{-1}, respectively, which is typical of a beidellitic smectite.

4.5. Thermal study

The results of the differential thermal analysis (DTA) and thermal gravimetric analysis (TGA) of the clays are shown in Fig. 9. DTA curves of the clays extracted from the altered rhyodacite reveal similarities in the low-temperature range. The thermograms show the following. (i) A pronounced endothermic peak system at low temperatures (<200 °C), which corresponds to the loss of hydration water. (ii) A strong endothermic peak appears at 510–513 °C, which is related to the presence of iron in the octahedral sites, which decreases the temperature. This peak has been reported in nontronite-type Fe-smectites. (iii) A dehydroxylation reaction that occurred at approximately 700 °C is followed by the S-form endo–exothermic reaction, which extends from 872 to 926 °C and is characteristic of Wyoming-type montmorillonite clays (Al, Fe). All of the thermal curves of the various samples showed a small peak at approximately 300 °C due to the presence of iron oxides. The TGA curves reveal a montmorillonite character and indicate three stages of mass loss at 100 °C, 150 °C and 500 °C. The first TG slope is related to the adsorption of water into the external surface and/or between the clay layers. As result of desorption and dehydratation reactions, there was a 2.25% loss in weight, which is less than that observed in similar source clay minerals (Guggenheim and Koster van Groos, 2001). This phenomenon could be related to the experimental conditions (in this study, the samples were dried at 60 °C before being placed into the crucible). The dehydration of the interlayer cations caused the second slope, which corresponded to a 0.95% loss in weight. The third weight loss (1.18%) can be mainly attributed to the dehydroxylation of smectitic clay.

4.6. Chemical analyses

The results of the chemical analysis (Table 1) show that the rhyodacitic lavas are characterised by silica supersaturation and Al_2O_3 excess. This high ratio of aluminium is reflected in the presence of normative corundum (Laridhi Ouazaa, 1994). The alumina saturation index (A/CNK) ($Al_2O_3/Ca_2O + Na_2O + K_2O$) varies between 1.8 and 2.29; this index (>1) gives these rocks a peraluminous character (Chappel and White, 1974; Clarke, 1981). An atypical potassium content (4%) was observed, which is typical of Oued Belif rhyodacites. Moreover, the analysis of REEs indicates that the Nefza acid rocks contain typical concentrations similar to the average chemical composition of Earth's crust (Halloul, 1989; Taylor

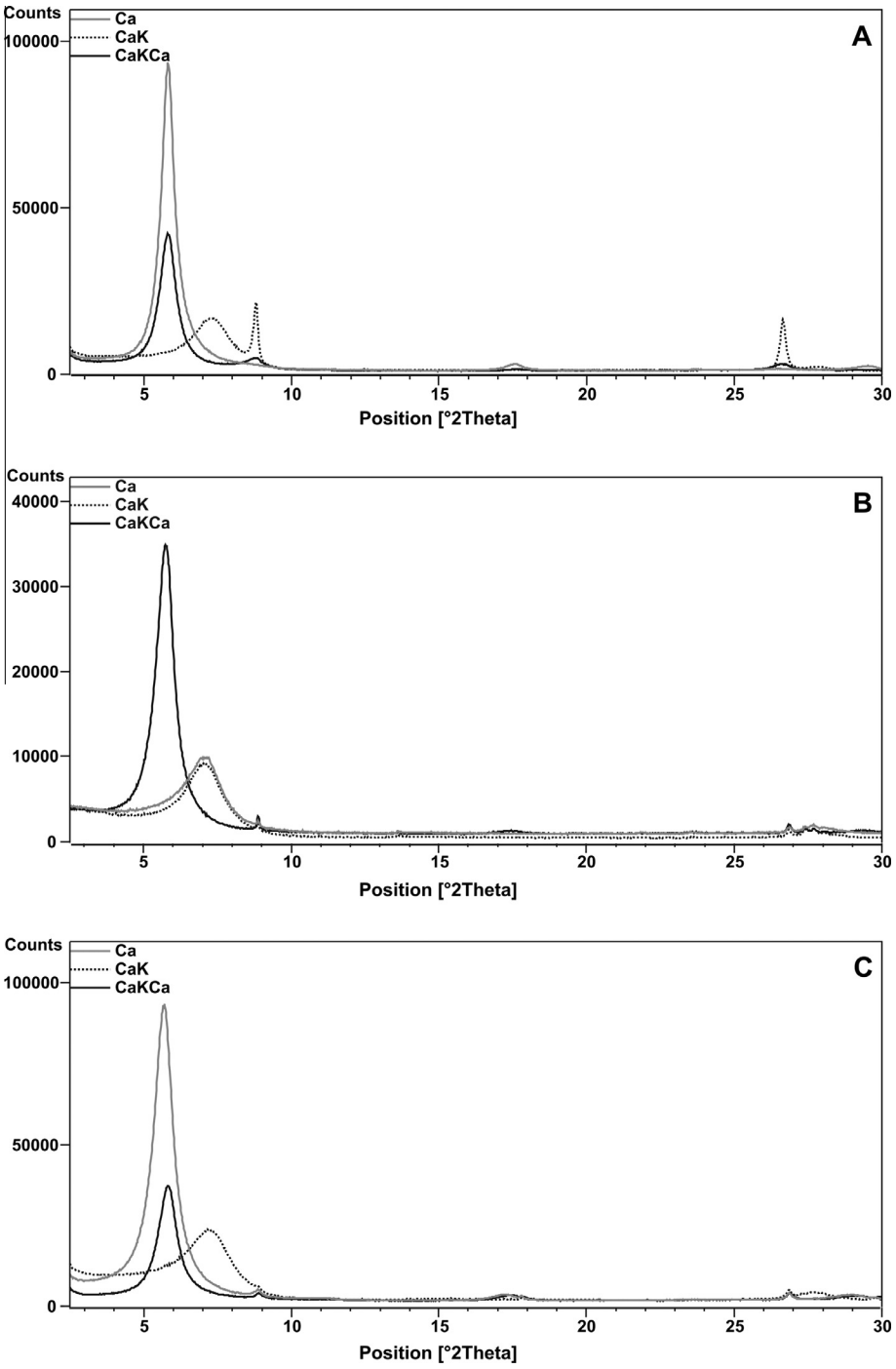

Fig. 7. XRD patterns of Ca, CaK, CaKCa-saturated samples of Oued Belif. (A) OB3; (B) OB6; (C) OB24.

and McLennan, 1981). The clay fractions isolated from the weathered rhyodacite show an alumino-ferriferous character, which is occasionally potassic.

The structural formulae of pure smectitic phases established from the punctual EDS analyses are given in Table 1.

The upper crust normalised REE patterns (normalisation value from Taylor and McLennan, 1981) show a strong enrichment of light REE (LREE) compared to heavy REE (HREE), and a negative anomaly in europium was observed for all samples (Table 2, Fig. 10). The comparison of the distribution curves of lanthanide for the entire rock and the clays shows an enrichment of the fine-fraction REE with a fractionation of LREE relative to HREE.

5. Discussion and conclusion

Petrographic investigation showed that the structure of the original rock is not preserved, which was confirmed by the intense alteration of plagioclase and biotite crystals. At the borders of the dome structure of the Oued Belif, we noted the presence of the ferruginous weathered products, which increases at the expense of ferromagnesian minerals (biotite), opaque minerals and glass, which evolve into clays. The conversion of magmatic glass to smectitic minerals has been described in several bentonitic deposits throughout the world (c.f., Christidis, 1998; Christidis and Dunham, 1997; Ddani et al., 2005).

Table 1
Chemical analyses of the major elements (%), loss on ignition (LOI) in weight %, cation exchange capacity (CEC), surface area (BET) of the rhyodacites, microprobe analyses of the associated clays and structural formulae based on $O_{10}(OH)_2$.

	RTOB3	AROB3	RTOB6	AROB6	RTOB24	AROB24
SiO_2	66.24	57.40	64.24	52.14	67.48	53.63
Al_2O_3	14.57	15.97	16.40	17.25	14.92	21.79
Fe_2O_3	3.39	7.99	3.23	9.76	2.49	6.97
MnO	0.038	0.015	0.018	0.004	0.035	0.00
MgO	1.17	3.15	1.35	1.93	0.98	1.98
CaO	1.68	0.74	2.51	0.88	1.94	2.02
Na_2O	2.84	0.75	3.00	1.79	3.34	1.76
K_2O	4.09	0.89	3.77	0.45	3.90	0.82
TiO_2	0.37	0.34	0.37	0.13	0.34	0.33
P_2O_5	0.13	0.35	0.18	0.05	0.093	0.00
LOI[a]	4.69		4.82		3.47	
Total	99.22		99.88		98.99	89.31
$(Al_2O_3 + Fe_2O_3)/MgO$	17.47	7.61	18.79	13.99	17.46	10.41
SiO_2/Al_2O_3	4.55	3.59	3.92	3.02	4.52	2.46
K_2O/Na_2O	1.44	1.19	1.26	0.25	1.17	1.46
Si		3.96		3.78		3.65
^{IV}Al		0.04		0.22		0.35
^{VI}Al		1.26		1.25		1.40
Fe^{3+}		0.42		0.53		0.36
Mg		0.32		0.21		0.20
Ti		0.02		0.01		0.02
Mn		0.00		0.00		0.00
Ca		0.05		0.07		0.15
Na		0.10		0.25		0.23
K		0.08		0.04		0.07
Tet. charge		0.04		0.22		0.35
Oct. charge		0.24		0.20		0.24
Interlayer charge		0.28		0.43		0.60
Layer charge		0.28		0.42		0.59
CEC (meq/100 g of dry clay)[b]		69.79		61		71
Surface area (m^2/g)[c]		80.08		54.55		53.14

[a] LOI – loss on ignition at 1000 °C; RT: bulk-rock; AR: clay fraction.
[b] Cation exchange capacity.
[c] Surface area determined by the method of Brunauer, Emett and Teller (BET).

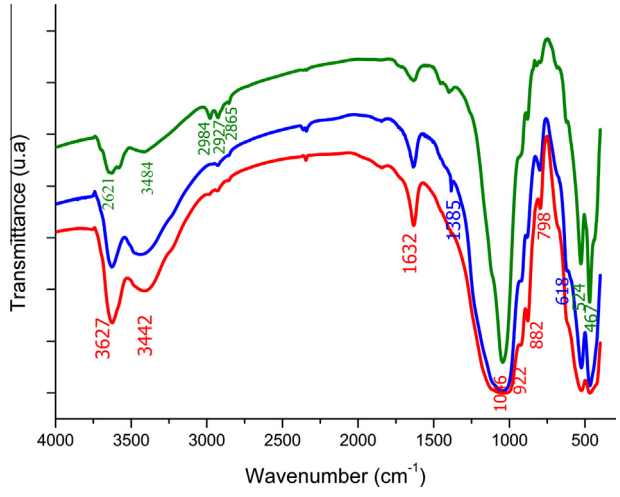

Fig. 8. Middle infrared (MIR) spectra of the clay samples (red curve: OB3; green curve: OB6 and blue curve: OB24). (For interpretation of the references to colour in this figure legend, the reader is referred to the web version of this article.)

The observation of altered rocks using optical microscopy revealed the presence of plagioclase crystals, which showed several dissolution cavities at the crystal edges and in the hub, where they form a dense network. These microcavities have been formed by the leaching of feldspar crystals by hydrothermal fluids that are then partially filled with neoformed phyllosilicates.

The XRD analysis of the clay fraction revealed an almost homogeneous mineral composition which, corresponds to a nearly smectitic phase with an insignificant amount of illite and kaolinite. The presence of illite and kaolinite suggests that they are derived from crystalline rocks that contained feldspar and mica. The presence of kaolinite and illite in the <2-μm fraction of the Oued Belif samples and the nature of the sheets (montmorillonitic or Beidellitic) caused a decrease in the CEC and external surface area values.

The nature of the swelling clay types was determined using IR spectroscopy, performed in support of the XRD analyses, to characterise the clay minerals. These results helped to confirm the alumino-ferriferous nature of the samples located in the distal part of the dome and the aluminous character of the samples nearest to the fresh rock.

Mineralogical and spectroscopic analyses were supplemented by differential thermal analysis. All samples presented similar thermal curves typical of smectitic clays. Clear differences were observed regarding the position, shape and intensity of the different peaks, which are attributed to the diversity of the saturating cations, which have different hydration energies.

The geochemical studies of both fresh and weathered rocks samples clearly indicated their peraluminous and potassic nature, which is linked to a crustal origin (Halloul, 1989; Laridhi Ouazaa, 1994) and to a potassic metasomatism (Talbi, 1998). The comparison of the chemical composition among the rhyodacites and the clays extracted from the weathered rocks showed a concentration of several chemical elements in the fine fraction (i.e., Al, K, Mg, Fe, Ca and Mn), which is clearly related to the leaching of these elements during the hydrothermal and supergene alteration of acidic lavas and their fastening in smectites (Christidis, 1998). The remarkably high content of aluminium in the fine fraction of the weathered rock may be due to the conversion of volcanic glasses into clay minerals (Altaner and Grim, 1990), whereas the relative mass increase of iron is undoubtedly due to the supply of iron from

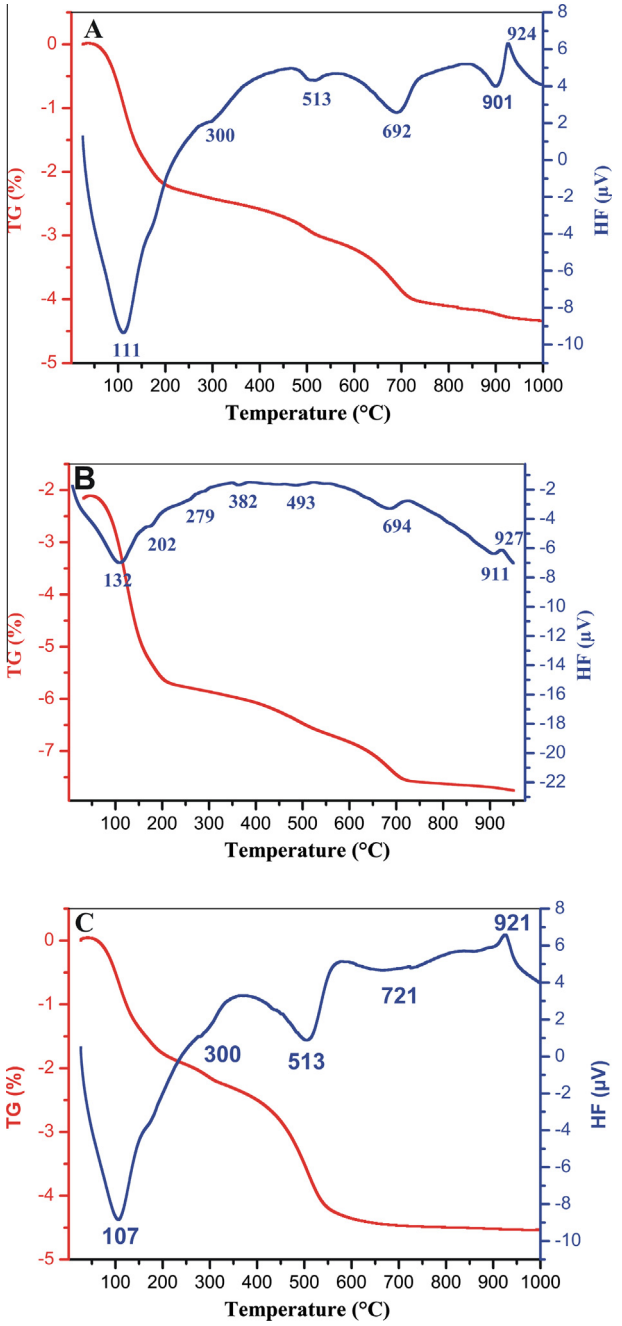

Fig. 9. TG–DTA curves of the clay samples (A) OB3; (B) OB6; (C) OB24.

the Tamra iron mine. Iron can also be derived from the pseudomorphose of the biotite. The enrichment of potassium can be attributed to the leaching of feldspars (Munch et al., 1996), which may contribute to the neoformation of illitic minerals. The distribution of the major and trace elements and REEs of the studied samples revealed variations what were closely related to the degree of rock weathering. It is well known that clays are the most important host minerals for REEs in alteration products (Kanazawa and Kamitani, 2006; Nyakairu et al., 2001; Roy and Smykatz-Kloss, 2007). Moreover, the important fractionation of LREEs compared with HREEs reflects the nature of these calco-alkaline lavas. However, the negative europium anomaly indicates the fractionation of plagioclase. The general shape of the curves for the lanthanide rhyodacitic lavas is characteristics of those clays.

The texture, primary mineralogy and alteration of the studied samples were characterised based on macroscopic and petrographic

Table 2
Chemical compositions of the trace and rare earth elements of rhyodacite and associated clay (ppm).

	RTOB3	AROB3	RTOB6	AROB6	RTOB24	AROB24	Upper crust
As	77.60	197	16.30	33.90	43.40	137	
Ba	1216	700	600	427	442	264	
Be	6.84	6.18	4.60	9.54	5.79	7.19	
Bi	1.26	1.92	0.16	0.39	1.20	6.55	
Cd	<l.d.	<l.d.	<l.d.	<l.d.	0.17	<l.d.	
Ce	77.50	72.0	84.60	15.00	78.70	99.20	33
Co	4.07	4.89	4.01	2.41	5.67	5.04	
Cr	13.10	6.40	13.10	10.80	14.70	14.10	
Cs	31.00	32.9	5.33	6.08	24.70	23.60	
Cu	<l.d.	20.6	8.30	15.00	7.80	28.50	
Dy	2.18	1.58	3.85	1.46	2.03	3.05	3.7
Er	1.08	0.721	1.71	0.673	1.03	1.26	2.2
Eu	0.875	0.550	1.310	0.258	0.947	0.986	1.1
Ga	24.30	23.8	27.60	30.00	24.70	21.60	
Gd	3.11	2.41	5.65	1.70	2.98	4.79	3.3
Ge	1.79	0.85	1.48	0.44	1.73	1.16	
Hf	4.70	1.96	4.98	2.53	4.74	1.32	
Ho	0.386	0.267	0.669	0.256	0.366	0.491	0.78
In	<l.d.	0.650	<l.d.	<l.d.	<l.d	0.34	
La	45.90	46.000	43.50	7.12	45.50	62.40	16
Lu	0.193	0.102	0.238	0.109	0.193	0.165	0.3
Mo	1.58	2.280	0.49	0.44	1.02	1.30	
Nb	13.9	10.900	13.7	5.99	13.3	5.76	
Nd	26.4	24.200	36.2	7.32	26.6	34.70	16
Ni	6.2	7.000	10.8	8.3	7.4	8.60	
Pb	77.7	152.000	44.4	18.2	106	615.	
Pr	7.98	7.150	10.1	1.92	8.05	9.72	3.9
Rb	331	79.300	139	16.4	279	52.50	
Sb	1.44	3.310	0.8	1.52	1.61	2.92	
Sm	4.71	4.450	7.42	1.89	4.54	7.38	3.5
Sn	7.32	8.920	6.11	9.53	5.82	9.66	
Sr	688	1831	400	120	564	1716	
Ta	1.44	1.340	1.53	1.05	1.42	0.67	
Tb	0.431	0.335	0.78	0.266	0.408	0.64	0.6
Th	20.7	19.400	23.5	9.63	24.4	19.10	
Tm	0.168	0.105	0.246	0.107	0.164	0.17	0.32
U	9.29	2.08	5.12	1.44	7.7	2.39	
V	32.9	23.50	38.2	45.3	34.4	42.90	
W	4.56	4.49	7.08	8.74	4.6	6.20	
Y	11.5	8.09	19.8	7.4	11.1	13.50	
Yb	1.21	0.691	1.57	0.743	1.21	1.18	2.2
Zn	129	1156	301	1008	197	1403	
Zr	175	50.5	182	46	177	32.20	

<l.d. – amount lower than the detection limits.
Normalisation was performed according to Taylor and Mclennan (1981).

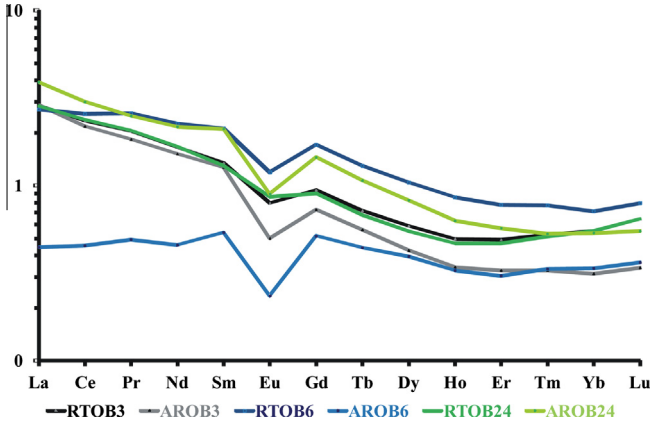

Fig. 10. Variation of the REE normalised to the crust of the Oued Belif rhyodacites and associated clays; normalisation was performed according to Taylor and Mclennan (1981).

observations. The transformations that affected the acid lavas mainly included ferrugination, silicification and clayey alteration.

The mineralogical study of the fine fraction of the studied samples showed that the cortege of clay minerals is homogeneous with an extremely slight variation depending on the sample location relative to the unaltered rock. This result therefore demonstrates that the nature of the clayey species depends on the intensity of the transformations that affect the rock. Generally, clays associated with acid volcanic rocks of Oued Belif are smectitic.

The supergene and hydrothermal alterations generated intermediate mineral species that have a similar intermediate character between the montmorillonitic and the beidellitic end-members. A similar example has been described in the Milos Island Greece, where the smectite was derived from acidic precursors and displayed significant compositional variations between beidellite and montmorillonite (Christidis and Dunham, 1993, 1997).

A less-intense alteration induced by hydrothermal processes primarily resulted in beidellite aluminous clays. Moreover, the distribution of major and trace elements and REEs of the investigated samples was used to characterise the chemical modifications subsequent to their emplacement. This chemical process mainly occurred as rare Earth leaching during lava alteration and their trapping in the clay fractions.

Acknowledgments

The first author (SD) extends his deep gratitude to Mr. Philippe Vieillard and Alain Meunier for their contribution to this research and HYDRASA-UMR 6532 CNRS for financing the chemical analyses of the clays and rocks. SD also thanks to Claude Fontaine for his invaluable recommendations when performing the analyses. Constructive comments from Ms. Najia Laridhi-Ouazaa are also highly appreciated. Sami Riahi and Najib Jammali are warmly acknowledged for their enjoyable company during the various field missions conducted in 2007 and 2009.

References

Abdelouahab, C., Ait Amar, H., Obretenov, T.Z., Gaid, A., 1988. Physicochemical and structural characteristics of some bentonitic clays for north-western Algeria. Analusis 16, 292–299.

Altaner, S.P., Grim, R.E., 1990. Mineralogy, chemistry, and diagenesis of tuffs in the Sucker Creek Formation (Miocene), eastern Oregon. Clays Clay Miner. 38, 561–572.

Bagdazarjan, G.P., Bajanic, S.D., Vass, D., 1972. Age radiométrique du volcanisme néogène dans le Nord de la Tunisie. Not. Serv. Géol. Tunisie 40, 79–93.

Bellon, H., 1976. Séries magmatiques néogènes et quaternaires du pourtour de la Méditerranée occidentale, comparées dans leur cadre géochronologique; implications géodynamiques. PhD thesis, Paris South University, France, p. 367.

Bouzouada, R., 1992. Géologie, Minéralogie et paragenèses des gîtes de fer du district des Nefza. Répartition des sulfures et des impuretés. Mémoire du diplôme des études approfondies en géologie, Université Tunis II, p. 77.

Chaftar, R., 1997a. Programme de reconnaissance par sondage mécanique; Ragoubet Es Seid. Rapport d'exécution des sondages. Mise au point (Rapport inédit O.N.M.).

Chaftar, R., 1997b. Programme de reconnaissance par sondage mécanique; Ragoubet Es Seid. Rapport d'exécution des sondages. Principaux résultats (Rapport inédit O.N.M.).

Chappel, B.W., White, A.J.R., 1974. Two contrasting granites types. Pac. Geol. 8, 173–174.

Christidis, G., 1998. Comparative study of the mobility of major and trace elements during alteration of an andesite and a rhyolite to bentonite, in the islands of Milos and Kimolos, Aegean, Greece. Clay Clay Miner. 46, 379–399.

Christidis, G., Dunham, A.C., 1993. Compositional variations in smectites: Part I. Alteration of intermediate volcanic rocks. A case study from Milos Island, Greece. Clay Miner. 28, 255–273.

Christidis, G., Dunham, A.C., 1997. Compositional variations in smectites: Part II. Alteration of acidic precursors, a case study from Milos Island, Greece. Clay Miner. 32, 253–270.

Clarke, D.B., 1981. The mineralogy of peraluminaous granites. A review. Can. Mineral. 19, 3–17.

Cohen, C.R., Schamel, S., Boyd-Kaygi, P., 1980. Neogene deformation in Northern Tunisia: origin of the Eastern Atlas by microplate-continental margin collision. Geol. Soc. Am. Bull. 91, 225–237.

Crampon, N., 1971. Etude géologique de la bordure des Mogods, du pays de Bizerte et du nord des Hédil. PhD thesis, Nancy I University, France, p. 522.

Ddani, M., Meunier, A., Zahraoui, M., Beaufort, D., El Wartiti, M., Fontaine, C., Boukili, B., El Mahi, B., 2005. Clay mineralogy and chemical composition of bentonites from the Gourougou volcanic massif (Northeast morocco). Clays Clay Miner. 53, 250–267.

Decrée, S., De Putter, Th., Yans, J., Recourt, Ph., Jamoussi, F., Bruyère, D., Dupuis, Ch., 2008a. Iron mineralization in Pliocene sediments of the Tamra iron mine (Nefza mining district, Tunisia): mixed influence of pedogenesis and hydrothermal alteration. Ore Geol. Rev. 33, 397–410.

Decrée, S., Marignac, Ch., De Putter, Th., Deloule, E., Liégeois, J.-P., Demaiffe, D., 2008b. Pb–Zn mineralisations in a Miocene regional extensional context: the case of the Sidi Driss and the Douahria ore deposits (Nefza mining district, N. Tunisia). Ore Geol. Rev. 34, 285–303.

Decrée, S., Marignac, Ch., De Putter, Th., Yans, J., Clauer, N., Dermech, M., Aloui, K., Baele, J.M., 2013. The Oued Belif hematite-rich breccias: a Miocene iron oxide Cu–Au (U-REE) deposit in the Nefza Mining District, Tunisia. Econ. Geol. 108, 1379–1396.

Dermech, M., 1990. Le complexe de l'Oued Bélif-Sidi Driss (Tunisie Septentrionale). Hydrothermalisme et métallogénie. Unpublished PhD thesis, Univ. Paris VI, France, p. 336.

Doumbouya, B., 1999. Caractérisation et exploitation des gîtes de fer du groupe Tamra Douaria-Boukchiba et de Jerisa (Tunisie Septentrionale). Mémoire de D. E. A., Univ. Tunis II, p. 115.

Faul, H., Foland, K., 1980. L'âge des rhyodacites de Nefza-Sedjenane. Notes du Service Géologique de Tunisie n°46. Trav. Géol. Tunisienne 14, 47–49.

Gottis, Ch., 1952. Les gisements de fer en Tunisie. In: Blondel, F., Marvier, L. (Eds.), Symposium sur les gisements du fer du monde, Tome I. XIXème Congrès Géologique International, pp. 211–222.

Gottis, Ch., Sainfeld, P., 1952. Les gîtes métallifères tunisiens. In: 19th International Geologycal Congress, Alger, Monographie Région, 2ème Série, 2 (104pp.).

Grim, R.E., Güven, N., 1978. Bentonites, Geology, Mineralogy, Properties and Uses. Developments in Sedimentology, vol. 24. Elsevier, Amsterdam.

Guggenheim, S., Koster van Groos, A.F., 2001. Baseline studies of the Clay Minerals Society Source Clays: thermal analysis. Clays Clay Miner. 49, 433–443.

Halloul, N., 1989. Géologie, pétrologie et géochimie du bimagmatisme néogène de la Tunisie Septentrionale (Nefza et Mogods). Implications pétrogénétiques et interprétation géodynamique. PhD thesis, Blaise-Pascal University, Clermont-Ferrand, France, p. 207.

Hofmann, U., Klemen, R., 1950. Verlust der Austauschfähigkeit von Lithiuminonen an bentonit durch Erhitzung. Z. Anorg. Allg. Chem. 262, 95–99.

Jallouli, C., Inoubli, M.H., Albouy, Y.Y., 1996. Le corps igné de Nefza (Tunisie septentrionale): caractéristiques géophysiques et discussion du mécanisme de sa mise en place. Not. Serv. Géol. Tunisie 62, 109–123.

Jolivet, L., Faccenna, C., 2000. Mediterranean extension and the African–Eurasia collision. Tectonics 19, 1095–1106.

Kanazawa, Y., Kamitani, M., 2006. Rare earth minerals in the world. J. Alloys Compd. 408, 1339–1343.

Kasaa, S., Laridhi-Ouazaa, N., Chaftar, R., Joron, J.L., Clocchiatti, R., Treuil, M., 2003. Relations entre les minéralisations et les roches magmatiques acides de la Tunisie septentrionale, exemple: la région de l'Oued Bélif. Not. Serv. Géol. Tunisie 70, 75–92.

Laridhi Ouazaa, N., 1994. Etude minéralogique et géochimique des épisodes magmatiques mesozoiques et miocenes de la Tunisie. Doctoral Thesis, Univ. De Tunis II, p. 466.

Mauduit, F., 1978. Le volcanisme néogène de la Tunisie continentale. PhD thesis, Univ. Paris Sud-Orsay, p. 148.

Meunier, A., Parneix, J.C., Beaufort, D., 1984. Les altérations hydrothermales des manifestations granitiques. Doc. BRGM 84, 131–143.

Moussi, B., 2012. Mode de genèse et valorisation de quelques argiles de la région de Nefza-Sejnane (Tunisie septentrionale). PhD thesis, Carthage University, p. 157.

Munch, P., Duplay, J., Cocheme, J.J., 1996. Alteration of silicic vitric tuffs interbedded in volcanoclastic deposites of the Southern Basin and Range Province, Mexico. Evidence Hydrotherm. React. 44, 49–67.

Negra, L., 1987. Pétrologie, minéralogie et géochimie des minéralisations et des roches encaissantes des basins associés aux structures tectoniques et magmatiques de l'Oued Bélif et du Jebel Haddada (Nord des Nefza, Tunisie septentrionale). Unpublished PhD thesis, Paris Sud University, France, p. 223.

Nyakairu, G.W.A., Koeberl, C., Kurzweil, H., 2001. The Buwambo kaolin deposit in Central Uganda: mineralogical and chemical composition. Geochem. J. 35, 245–256.

Ould Bagga, M., Abdeljaoued, S., Mercier, E., 2006. La «Zone des nappes» de Tunisie : une marge méso-cénozoique en blocs basculés modérément inversée (région de Tabarka Jendouba, Tunisie nord-occidentale). Bull. Soc. Géol. France 177, 145–154.

Perthuisot, V., 1978. Dynamique et pétrogenèse des extrusions triasiques en Tunisie septentrionale. Doctoral thesis, Paris, Ecole Nationale Supérieure, p. 321.

Petit, S., Robert, J.L., Decarreau, A., Besson, G., Grauby, O., Martin, F., 1995. Apport des méthodes spectroscopiques à la caractérisation des phyllosilicates 2:1. Bull. Cent. Rech. Explor. Prod. Elf Aquitaine 19, 119–147.

Riahi, S., Soussi, M., Boukhalfa, K., Ben Ismaïl Lattrache, K., Stow, D., Khomsi, S., Bedir, M., 2010. Stratigraphy, sedimentology and structure of the Numidian Flysch thrust belt in northern Tunisia. J. Afr. Earth Sci. 57, 109–126.

Rouvier, H., 1977. Géologie de l'extrême Nord Tunisien: tectonique et paléogéographie superposées à l'extrémité orientale de la chaîne Nord-Maghrebine. PhD thesis, Pierre et Marie Curie University, Paris, France, p. 215.

Rouvier, H., 1987. Carte géologique de la Tunisie; feuille n°10: Nefza. Service Géologique, Office National des Mines.

Rouvier, H., 1988. Notice explicative de la carte géologique de la Tunisie au 1/50000e Nefza, feuille 10. Office National des Mines, Direction de la Géologie, p. 51.
Roy, P.D., Smykatz-Kloss, W., 2007. REE geochemistry of the recent playa sediments from the Desert, India: an implication to playa sediment provenance. Chem. Erde – Geochem. 67, 55–68.
Sainfeld, P., 1952. Les gîtes plombo-zincifères de Tunisie. An. Mines Géol. 9, 285.
Sato, T., Watanabe, T., Otsuka, R., 1992. Effets of layer charge location, and energy change on expansion properties of dioctahedral smectites. Clays Clay Miner. 40, 103–113.
Schultz, L.G., 1969. Lithium and potassium absorption, dehydroxylation temperature, and structural water content of aluminous smectites. Clays Clay Miner. 17, 115–149.
Sghaier, D., 2005. Les argiles de la région de l'Oued Bélif entre l'héritage et la néoformation (Tunisie septentrionale). Mém. Mastère. Univ. Tunis II, p. 165.
Talbi, F., 1998. Pétrologie, Géochimie, études des phases fluides et gîtologie liées au magmatismes néogène de la Tunisie septentrionales. Doctoral Thesis, Univ. Tunis II, p. 368.
Talbi, F., Slim-Shimi, N., Tlig, S., Zargouni, F., 1999. Nature, origine et évolution des fluides dans le district minier de la caldeira d'Oued Bélif (Nefza, Tunisie septentrionale). C. R. l'Académie Sci. Paris, Sci. Terre Planèt. 328, 153–160.
Talbi, F., Jaafari, M., Tlig, S., 2005. Magmatisme néogène de la Tunisie septentrionale: pétrogenèse et événements géodynamiques. Rev. Soc. Geol. España 18, 241–252.
Taylor, S.R., McLennan, S.M., 1981. The composition and evolution of the continental crust: rare earth element evidence from sedimentary rocks. Philos. Trans. R. Soc. Lond. A301, 381–399.
Tlig, S., Erraoui, L., Ben Aissa, L., Alouani, R., Ali Tagorti, M., 1991. Tectogenèses alpine et atlasique: deux événements distincts dans l'histoire géologique de la Tunisie Corrélation avec les événements clés en Méditerranée. C. R. l'Académie Sci. Paris 312, 295–301.
Yaich, C., 2000. Corrélation stratigraphique entre les unités Oligo-Miocènes de Tunisie centrale et le Numidien. C. R. l'Academie Sci. Paris – Ser. IIA-Earth Planet. Sci. 331, 499–506.